RSC Advances

PAPER

View Article Online
View Journal | View Issue

Cite this: *RSC Adv.*, 2021, **11**, 38189

Synthesis of fluorinated phosphorus-containing copolymers and their immobilization and properties on stainless steel†

Farzana Kousar and Stephen C. Moratti*

Received 31st July 2021
Accepted 22nd November 2021

DOI: 10.1039/d1ra05813d

rsc.li/rsc-advances

A series of fluorinated-phosphonic acid methacrylates were synthesized by free radical polymerization using heptadecafluorodecyl methacrylate (HDFDMA) and (dimethoxyphosphoryl) methyl methacrylate (DMPMM) monomers for potential application as anti-corrosion coatings. The dimethyl protecting groups were then hydrolyzed, giving phosphonic acid groups that are able to stably bind onto metal oxide surfaces. The copolymers were then immobilized as a monolayer film to the surface of 316L stainless steel by treatment of dilute solutions in trifluoroacetic acid for 30 minutes followed by rinsing. The surfaces were analyzed using various techniques and contact angles as high as 128° were recorded for some copolymer functionalized surfaces. Results also demonstrated that the polymer films proved stable to hydrolysis over several weeks of immersion in water.

Introduction

Fluoropolymers are widely used because of their exceptional properties, including high thermal, and weather resistance, excellent stability towards solvents and aggressive chemicals, and low surface energy. They also possess low values of dielectric constant, flammability, refractive index, and moisture absorption. As a result, they have found applications in many industries including construction, automotive, petrochemical, aerospace, chemical engineering, optics, textile treatment, and microelectronics.[1,2]

Phosphorus-containing monomers and polymers have also attracted the interest of the materials community due to their useful properties such as metal chelation and fire retardancy.[3–5] The resulting polymers have been employed in a wide range of applications including biomedicine,[5,6] metal complexation,[7] fuel cell membranes,[8] superlubricity coatings,[9] and anti-corrosion coatings.[10–12] Any anticorrosion coating must stick to the substrate well in the presence of high humidity or water (wet adhesion).[10] Of particular interest here is the strong affinity of the phosphate/phosphonate group for metal ions and metal oxide surfaces.[13] Results from our previous work have shown that phosphonate based copolymers have shown stable monolayer binding to 316L stainless steel substrate under aqueous conditions.[14] As stainless steel is widely used in industry and medicine, the modification of its surface properties is of great interest. The formation of ultrathin stable monolayers has an added attraction of being able to allow heat and light transfer while affecting the binding properties of molecules such as proteins. The copolymerization of fluorinated monomers with other co-monomers has gained a lot of interest.[15,16] The co-monomers can possess functional groups such as hydroxyl, ester, ether,[17] acetoxy,[18] or carboxylic acid.[2] Because the presence of fluorine atoms on the backbones of polymers or on a spacer connecting to this backbone can change the electron density of nearby functional groups, thus improving certain properties of the resulting copolymers[19,20] such as proton conductivity,[21] thermal stability,[22] or hydrophobicity[22] as compared to the pristine homopolymer.

To incorporate phosphorus-containing functionality into polymers, two main methods have been used. The first involves the chemical modification of existing polymers by processes such as phosphorylation.[23] Alternatively, phosphorus-containing vinyl monomers can be polymerized and copolymerized,[24] including methacrylates,[25] methacrylamides,[25] vinyl phosphonic acid, and styrenic and allylic monomers.[26–28] A wide range of phosphonated fluorinated polymers are known.[19,20] For instance, Timperley *et al.*[29] synthesized polymers with bis(-fluoroalkyl)acrylic and methacrylic phosphate functionalities for flame retardant applications. Tayouo *et al.*[30] prepared fluorinated copolymers with phosphonic acid side functionalities for new membranes that could be used in fuel cells. Banerjee *et al.*[31] has used poly(vinylidene fluoride) containing phosphonic acids as thick anticorrosion coatings for steel. Labalme *et al.*[32] prepared a series of membranes made from poly(-vinylidene fluoride-*co*-chlorotrifluoroethylene) and a fluorinated copolymer containing phosphonic acid to increase

Department of Chemistry, The University of Otago, Dunedin, 9010, New Zealand. E-mail: smoratti@chemistry.otago.ac.nz

† Electronic supplementary information (ESI) available: ^{1}H, ^{31}P and ^{19}F NMR spectra, FTIR and TGA traces. Contact angles, and XPS measurements on uncoated and polymer immobilized stainless steel. See DOI: 10.1039/d1ra05813d

thermo-chemical stability and mechanical proton exchange membrane capabilities.

1*H*,1*H*,2*H*,2*H*-Heptadecafluorodecyl methacrylate (HDFDMA) is a commercially available monomer that has been used previously to prepare low surface energy materials.[33–35] To copolymerize this HDFDMA directly with phosphonate monomers is challenging because of the great difference in polarities. To get around this in this work, we use a protected phosphonate monomer (dimethoxyphosphoryl)methyl methacrylate (DMPMM), that can be subsequently deprotected after polymerization. Furthermore, the polymers were synthesized and immobilized on stainless steel surfaces. The polymer immobilized surfaces were then analyzed by static water contact angle measurements, attenuated total reflectance infrared, and X-ray photoelectron spectroscopy. The overall concept used in this study is shown in Fig. 1.

Results and discussion

Synthesis

There are a few reports on the homopolymerization of heptadecafluorodecyl methacrylate (HDFDMA), using AIBN as an initiator in supercritical carbon dioxide.[36,37] Canniccioni *et al.*[25] reported the synthesis of (dimethoxyphosphoryl)methyl methacrylate (DMPMM) homopolymer by RAFT polymerization and Solimando *et al.*[38] by nitroxide-mediated polymerization. There are no reports of their copolymerization. In this work, homopolymers of 1*H*,1*H*,2*H*,2*H*-heptadecafluorodecyl methacrylate (poly(HDFDMA)) and (dimethoxyphosphoryl)methyl methacrylate (poly(PMM)) were synthesized using free radical polymerization.

Poly(HDFDMA) synthesis

The homopolymer was synthesized in 1,4-dioxane by using AIBN as an initiator (Fig. S1 and S2†). In a typical polymerization, all the reactants were mixed, degassed, and heated at 85 °C for 24 h. The conversion of monomers to polymer was measured by ^{1}H NMR spectroscopy and the resultant polymer was purified by precipitation into hexane. A fluffy solid was obtained in good yield (86%), which was soluble in hexafluoroisopropanol (HFIP) and trifluoroacetic acid (TFA), but not in normal organic solvents. To confirm the chemical structure of the polymer, a ^{1}H NMR spectrum was measured in deuterated trifluoroacetic acid (CF_3CO_2D) as shown in Fig. S1.† No sign of residual monomer was observed in the spectrum.

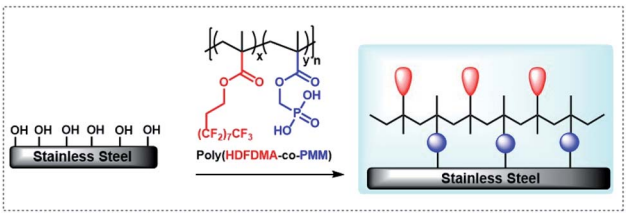

Fig. 1 Adsorption of poly(HDFDMA-*co*-PMM) copolymer onto the metal (hydr)oxide surface layer of stainless steel.

Poly(PMM) synthesis

The reaction consists of two stages. In the first stage, a homopolymer of protected polymer (phosphonate ester) was prepared in good yield (86%). In the second stage, the obtained phosphonate ester is reacted with trimethylsilyl bromide and then methanol to deprotect the phosphonate ester into a phosphonic acid group. The ^{1}H NMR spectra of the monomer, and the protected and deprotected polymer are shown in Fig. S3.† Broad peaks at 2.2–1.9 and 1.2–0.8 ppm were attributed to protons of the polymer backbone (CH_2 and CH_3 groups, respectively) of the protected polymer (Fig. S3(b and c)),† whereas signals at 4.2–4.4 ppm corresponding to the methylene in a-position of the phosphorus atom.

After deprotection, the signals corresponding to the methyl ester groups disappeared, as shown in Fig. S3(c).† Protons of the methylene in the a-position of the phosphorus atom were found to shift to 4.25–4.0 ppm in the deprotected polymer. To further confirm the deprotection, a ^{31}P NMR spectrum was taken for both protected and deprotected polymers as shown in Fig. S4.† The spectrum showed a signal at 21.0 ppm, characteristic of a phosphonate ester group (Fig. S4(a)†). In the deprotected poly(PMM) polymer spectrum as shown in Fig. S4(b),† the phosphorous signal showed a shift of the signal from 21.0 to 15.4 ppm.

Poly(HDFDMA-*co*-PMM) synthesis

Next, copolymers of these two monomers were prepared similarly in five ratios (HDFDMA : DMPMM as 3 : 1, 1 : 1, 1 : 2, 1 : 3, and 1 : 4 (Scheme 1c)). These will be denoted in the text as poly(HDFDMA-*co*-PMM)-[3 : 1] or simply as [3 : 1] *etc.* The ^{1}H NMR analysis of the [1 : 1] copolymer before and after deprotection is shown in (Fig. 2). The formation of poly(HDFDMA-*co*-DMPMM) copolymer with mol ratio [1 : 1] was confirmed by ^{1}H NMR analysis in deuterated trifluoroacetic acid (Fig. 2(a)) by comparing the signals of the reactive double bond to the signals of the methylene in a-position of the phosphonated ester group at 4.14–4.78 ppm. Successful polymerization was confirmed with the disappearance of the double bond signals (5.62 and 6.13 ppm) and the appearance of broad signals of the methacrylate backbone 2.0–2.5 and 0.80–1.45 in the ^{1}H NMR (Fig. S5†). A doublet present at 4.0–4.2 ppm corresponds to the two $(CH_3O)_2$–P groups from the DMPMM phosphonate (Fig. 2(a)). It is presumed that the copolymerization is statistical in nature and samples of polymer isolation at early stages had very similar NMR spectra to the final material and so showed little obvious composition drift.

Deprotection of phosphonated ester groups

The phosphonate ester groups were silylated using TMS-Br and then hydrolyzed with methanol to obtain the desired phosphonic acid groups. The resulting hydrolyzed poly(HDFDMA-*co*-PMM) was characterized by ^{1}H NMR spectroscopy in deuterated TFA, which showed the disappearance of the signal corresponding to the protons of the methyl ester groups as shown in Fig. 2(b), with the rest of the spectra remaining similar.

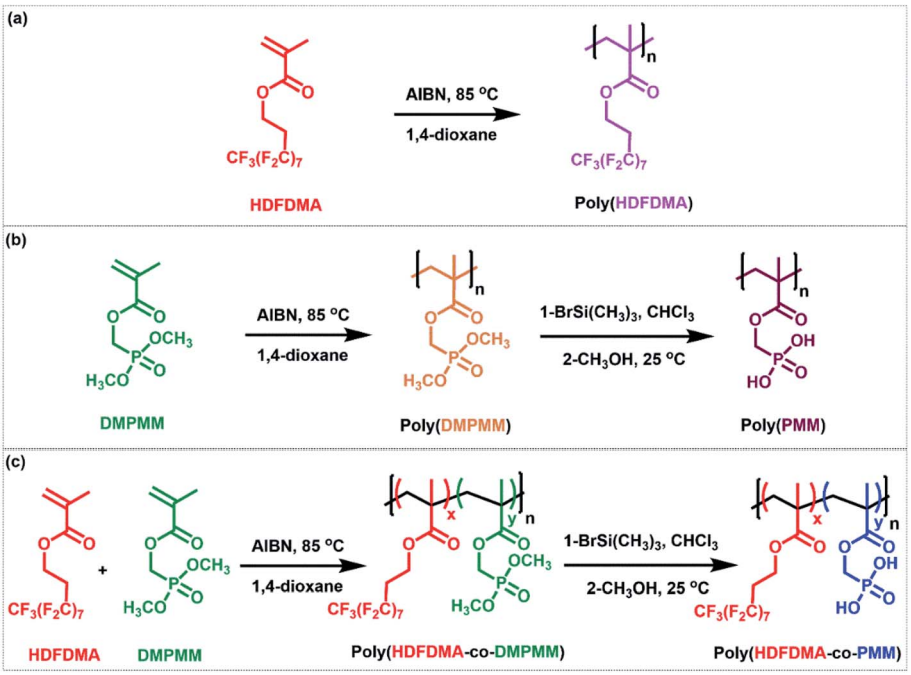

Scheme 1 The preparation of (a) poly(HDFDMA) homopolymer, (b) poly(PMM) homopolymer, and (c) fluorinated poly(HDFDMA-*co*-PMM) copolymer.

The deprotection was also validated using ^{31}P NMR (Fig. 3), spectroscopy which showed a shift in the signal from 31.9 to 28.0 ppm. Additionally, no residual signal of unprotected or mono-deprotected phosphonic acid (usually observed between the signals of protected and deprotected groups) was observed. ^{31}P NMR spectra were taken for all molar ratios and no difference in the peak position and distribution was noticed. ^{19}F NMR spectra further support the successful copolymerization. A broadening of the fluorine resonances was observed in the poly(HDFDMA-*co*-PMM) copolymer spectrum (Fig. S6(b)†) as

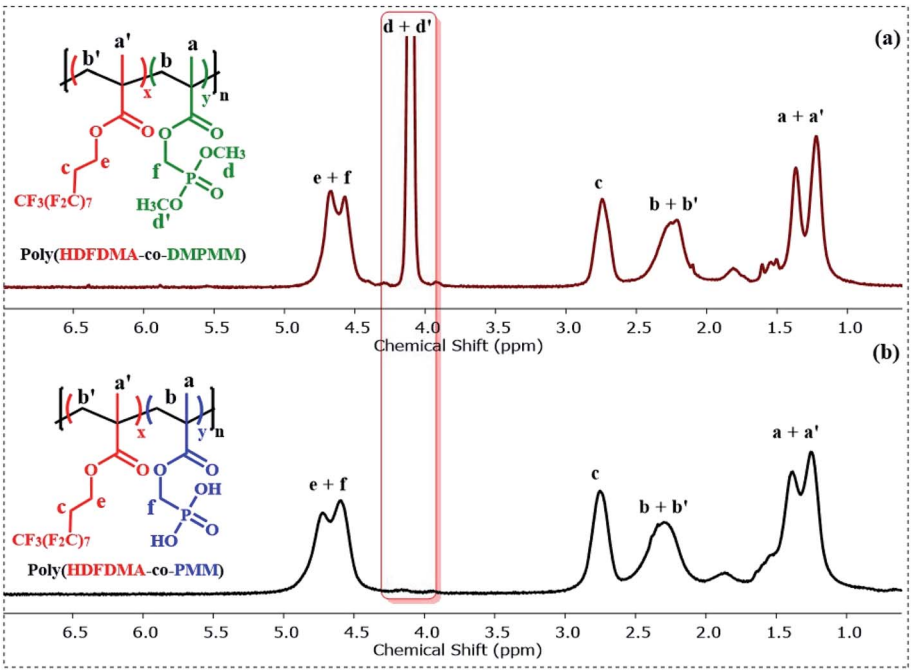

Fig. 2 (a) ^{1}H NMR (400 MHz) spectra in CF_3CO_2D of poly(HDFDMA-*co*-DMPMM) protected copolymer with mol ratio [1 : 1], and (b) the resulting deprotected poly(HDFDMA-*co*-PMM) copolymer.

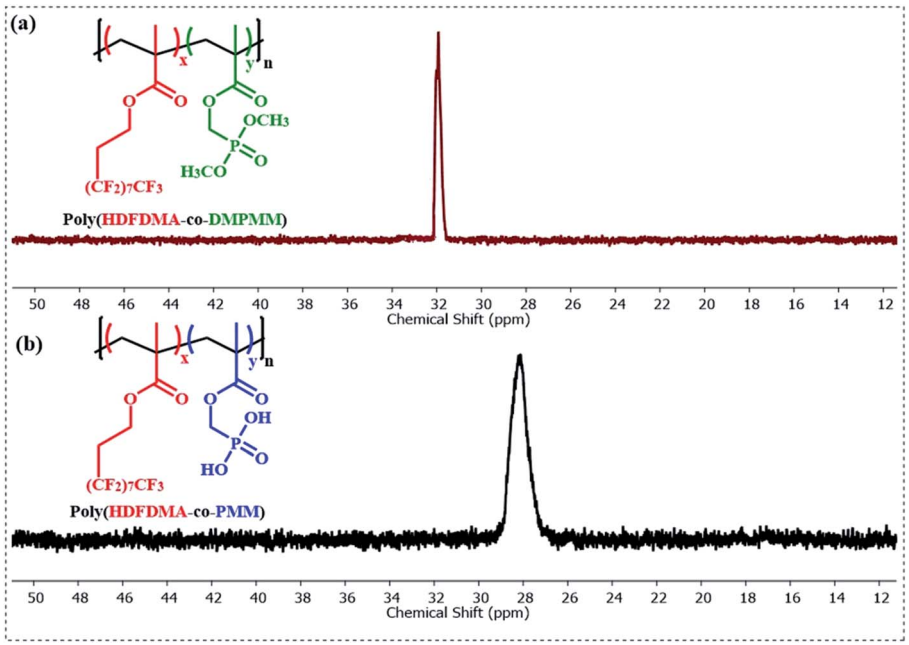

Fig. 3 (a) ^{31}P NMR (400 MHz) spectra of poly(HDFDMA-*co*-DMPMM) protected copolymer, and (b) the resulting hydrolyzed (deprotected) poly(HDFDMA-*co*-PMM) copolymer for mol ratio [1 : 1]. Both spectra were taken in deuterated trifluoroacetic acid (CF_3CO_2D).

compared to the monomer (Fig. S6(a)†), which corresponds to the CH_2–CF_2 functional group, together with a small shift.

Solubility

The deprotected poly(PMM) was soluble in polar solvents such as water, methanol, ethanol, acetonitrile, DMSO, and DMF, but insoluble in TFA and hexafluoroisopropanol (HFIP). The poly(-HDFDMA) homopolymer was soluble in chloroform and TFA. The poly(HDFDMA-*co*-DMPMM) deprotected copolymers in all mol ratios were soluble in TFA, and they were found to swell in DMF and DMSO at room temperature, and appeared slightly soluble. In NaOH solution, these copolymers formed stable and cloudy dispersions.

Gel permeation chromatography

In the case of typical fluorinated copolymers, it is often difficult to determine a molecular weight using GPC because of their poor solubility by suitable solvents. So molecular weights were measured on the protected polymers which were soluble in $CHCl_3$ as given in Table 1. The obtained degrees of polymerization are reasonable for such hindered monomers, with about 20–40 monomers per chain. No obvious trend could be observed on changing the relative amounts of each monomer.

Thermogravimetric analysis

The thermal stabilities of the polymers were evaluated using TGA under a nitrogen atmosphere. The TGA curves for the homopolymers and poly(HDFDMA-*co*-PMM) copolymer with mol ratio [1 : 1] are shown in Fig. 5, and other mol ratios in the ESI (Fig. S7†). Poly(PMM) exhibits an initial weight loss of about 7% at temperatures around 93 °C which probably reflects a loss of water due to the condensation of two adjacent phosphonic acid groups leading to a phosphonic anhydride as reported by other authors[30] (Fig. 5). The resulting polymer is still soluble, suggesting that the condensation is mainly intramolecular. In the case of the fluorinated copolymers, there was no initial weight loss observed in the TGA curve before 200 °C. This lack of apparent anhydride formation in the copolymers probably reflects that the phosphonate groups are less likely to be adjacent in the chain. Both the homopolymers poly(PMM) and poly(HDFDMA) decomposed in two steps.

For poly(PMM), the weight loss was relatively steep in the first step starting from 228 to 298 °C, and more gradual in the second step (298–633 °C). Poly(HDFDMA) showed the first 55% weight loss at 167–299 °C, and the second from 299–441 °C with a 45% loss of polymer.

These types of multi-step thermograms are commonly found in methacrylate polymers, where the chains that terminate by combination are much less thermally stable than those that terminate by disproportionation.[39] Poly(HDFDMA) showed complete degradation at high temperatures compared to poly(PMM) which showed a 38% residue. This may be due to the formation of involatile polyphosphate products in the latter. The copolymers showed intermediate behavior, with the residue amount mirroring the proportion of phosphonate in the polymer.

IR spectroscopy

The homopolymers and copolymers were examined using IR spectroscopy as shown in Fig. 4. The peak at 1732–1734 cm^{-1} is

Table 1 The various polymers as prepared through free-radical polymerization with varying monomer mol ratios[a]

S. no.	Polymers	Mol ratio HDFDMA to DMPMM	Conversion (%)	M_n (g mol^{-1})	M_w (g mol^{-1})	Molar mass dispersities
1	Poly(HDFDMA)	[1 : 0]	84	12 912	27 659	1.14
2	Poly(DMPMM)	[0 : 1]	85.4	16 123	46 668	1.8
3	Poly(HDFDMA-*co*-DMPMM)	[3 : 1]	95.4	6875	8250	1.2
4	Poly(HDFDMA-*co*-DMPMM)	[1 : 1]	96.7	19 502	29 464	1.51
5	Poly(HDFDMA-*co*-DMPMM)	[1 : 2]	96.6	17 780	32 558	1.83
6	Poly(HDFDMA-*co*-DMPMM)	[1 : 3]	94.9	8398	88 874	1.3
7	Poly(HDFDMA-*co*-DMPMM)	[1 : 4]	90.7	8023	66 590	1.6

[a] The polymerization time for all the polymerization processes was 24 h. AIBN (1 wt%) was used as an initiator, 1,4-dioxane as a solvent, and polymerization was carried out at 85 °C.

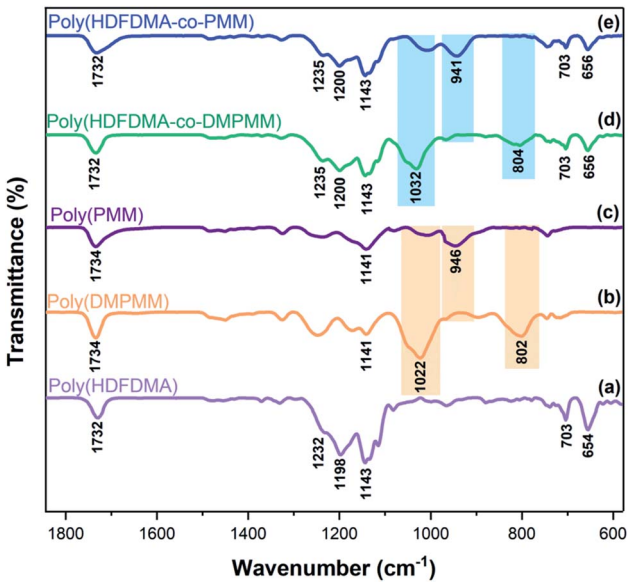

Fig. 4 (a) ATR-IR spectrum of poly(HDFDMA) homopolymer, (b) protected poly(DMPMM) homopolymer, (c) deprotected poly(PMM) homopolymer, (d) protected poly(HDFDMA-*co*-DMPMM) copolymer [1 : 1], and (e) deprotected poly(HDFDMA-*co*-PMM) copolymer [1 : 1].

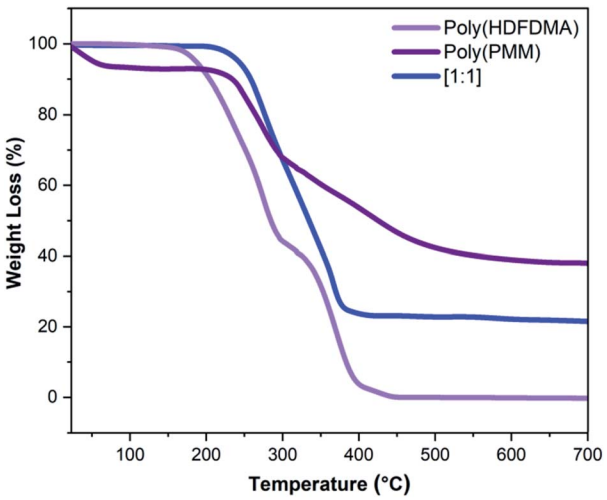

Fig. 5 TGA thermograms of poly(HDFDMA) homopolymer, poly(PMM) homopolymer, and poly(HDFDMA-*co*-PMM) copolymer with mol ratio [1 : 1] heated at 10 °C min^{-1} under nitrogen.

associated with C=O stretching peaks. Ester groups usually show two C–O stretches at around 1250 and 1100 cm^{-1} regions.

For fluorinated polymers, the symmetric and asymmetric stretching vibrations of C–F (1201 cm^{-1} and 1150 cm^{-1} in Teflon), overlap with the C–O stretches.[40] Two medium intensity bands appeared at 656 and 703 cm^{-1} resulting from a combination of rocking and wagging vibrations of the CF_2 groups.[41]

The presence of the dimethyl phosphonate ester groups in poly(PMM) and poly(HDFDMA-*co*-PMM) polymers was shown by the strong absorbances associated with the P–O–CH_3 stretching bands at 1022–1032 cm^{-1}.[42,43] The peaks near 802–804 cm^{-1} are also associated with P–O–CH_3 stretching. The successful complete hydrolysis of such phosphonate esters was confirmed by the disappearance of the P–O–CH_3 stretching bands and the appearance of the P–OH stretch at 946–941 cm^{-1}.[38]

Immobilization of polymers

The idealized process of showing the adsorption and interaction of phosphonates with stainless steel has been studied in our previous work.[14,44] The adhesion was determined to be *via* covalent metal-phosphonate linkages, and it assumed that the same binding is found here. The thickness could not be determined directly as in previous work as QCM-D measurements were not possible in the aggressive solvents used here. Ellipsometry gave unreliable results, probably due to the large surface roughness and heterogeneity of the SS surface. However, the stability of the films suggests covalent binding, which is only possible for a polymer monolayer.

The surface properties of the polymer films formed on stainless steel coupon surfaces were examined by static water contact angle (SCA) measurements. Results revealed that the as-received uncleaned SS (AR-SS) coupon surface showed a CA of 87 ± 4° which is comparable to that reported in the literature.[45] In contrast, the sulfochromic acid cleaned SS coupon surface was much more hydrophilic, exhibiting a high CA value of 18 ± 4°. Exposure of the cleaned SS coupon surface to TFA solution for 30 minutes did not change the contact angle (17 ± 4°),

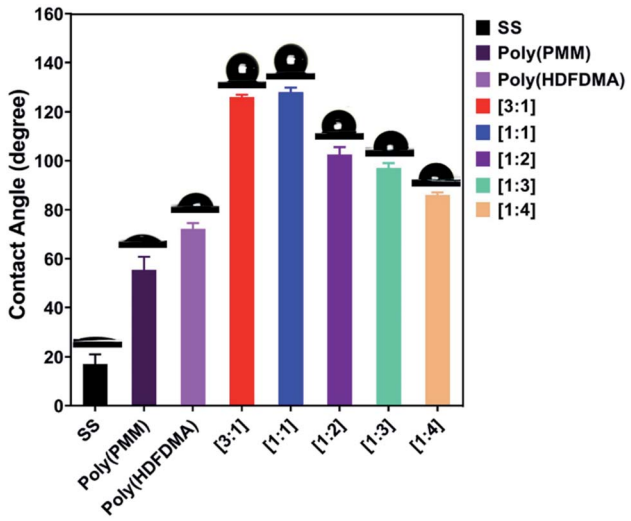

Fig. 6 Contact angles of uncoated and polymer coated SS coupon surfaces cleaned with sulfochromic acid solution. The polymers were deposited from TFA at a concentration of 1 wt% of the polymer solution. Data are presented as mean ± standard deviation ($N = 3$).

showing that the solvent for the polymers was not influencing the results (see Fig. S8 and Table S1†).

The cleaned SS coupon surfaces were treated with dilute (10 mg mL^{-1}) solutions of the polymers in TFA (except poly(PMM) in water at pH 3.0). Exposure to poly(PMM) phosphonic acid homopolymer gave a CA of 55 ± 5° on SS surface, suggesting some adsorption. A higher CA of about 72 ± 2° was observed for the fluorinated homopolymer poly(HDFDMA). However, a significant increase in CA was observed for the poly(HDFDMA-*co*-PMM) copolymers, which indicates a higher degree of adsorption due to the presence of the phosphate coordinating ligands. The [1 : 1] copolymer gave the most hydrophilic surface with a CA of 128 ± 2° as shown in Fig. 6. As the ratio of fluorinated monomers decreased in the copolymers, so did the measured contact angle. The CA value for the [1 : 1] polymer on SS is very high for a non-textured polymer film. For instance, Teflon (PTFE) with a smooth surface has an advancing contact angle in the range of 108°–112° (ref. 46–48) but for a rough surface, the values are higher with advancing and receding contact angles, of 128°/78°.[49] This suggests that the steel roughness (0.8 μm as stated by the supplier) is helping to increase the CA in the adsorbed polymer films. Nevertheless, this high contact angle suggests complete coverage of the steel surface by the fluorinated copolymers. Copolymers with mol ratios [1 : 2], [1 : 3], and [1 : 4] were also deposited on SS surfaces from dilute dimethylsulfoxide (DMSO) and comparable contact angles were observed despite their low solubility compared to TFA (see Fig. S10(a)†). We showed in previous work,[14] that a PEO-phosphonate copolymer film deposited from water only formed a monolayer on stainless steel as measured by QCM-D.

We assume in this case that the same is true as these films are invisible to the eye. Unfortunately, QCM-D was not practical with the organic solvent used here (TFA) and we have found that our stainless steel surfaces are too rough to give reliable results by ellipsometry.

Instead, we carried out IR to give some indication (Fig. S11†). Very faint signals resulting from C–F and C–O stretches between 1100–1250 cm^{-1} could be seen on coated steel surfaces, though the carbonyl stretch appeared shifted to *ca.* 1650 cm^{-1}, indication some coordination to the surface. The intensity is similar to that observed with the previous PEG-phosphonate polymers, suggesting a polymer monolayer. This very thin coating might be advantageous in many applications such as food processing, as it can allow ready heat transfer to occur, while still modifying the surface characteristics.

X-ray photoelectron spectroscopy

XPS was used to further analyze the bonding motif, the chemical states, and composition of elements of clean uncoated and polymer coated SS coupon surfaces. A typical XPS survey spectrum of uncoated SS coupon is presented in Fig. S12 (a) in the ESI,† which exhibits intense C, O, and Cr peaks, and shows the absence of fluorine and phosphorus, as expected. The large C percentage is typically ascribed to adventitious surface contamination that is very difficult to avoid. For all the polymer-coated SS coupons, the spectra (Fig. S12(b–d)†) showed the presence of carbon, oxygen, and chromium. However, the presence of fluorine, in poly(HDFDMA)-coated samples and phosphorus in poly(PMM)-coated samples were detected. The results for the copolymers showed that both fluorine and phosphorus were present.

A significant increase in the atomic percentage of carbon was observed on the polymer coated coupon surfaces relative to uncoated SS due to the carbon content of the polymers. As expected, the maximum phosphorus adsorption was observed from the poly(PMM) homopolymer and the least from the [3 : 1] mol ratio copolymer. The F 1s signal was detected in all fluorinated polymers but its concentration was lower in poly(HDFDMA) homopolymer compared to the copolymers, showing its poorer overall adsorption without the phosphonate linker. The fluorine signal was noticed to increase as the mol ratio increased from [1 : 4] to [1 : 1] copolymer as would be expected. The measured intensity of Cr and other metals such as Fe were decreased after the deposition of polymers, as the technique only measures the top nm or so of the metal which is now composed mainly of polymer. To investigate closely the possible speciation of coated SS surfaces, core level scans for C 1s, F 1s, P 2p, and O 1s were carried out.

C 1s core level scan

The core level scans for C 1s species of uncoated SS, poly(PMM), and poly(HDFDMA) homopolymers, and poly(HDFDMA-*co*-PMM) copolymer with mol ratio [1 : 1] coated SS coupons are shown in Fig. 7, and in Fig. S13† for other mol ratios of copolymers.

Usually, the carbon component signal is regarded as the combination of the carbon alloy in stainless steel and surface contaminants formed in the air.[50] To accurately determine the functional groups, the C 1s peak is deconvoluted into various

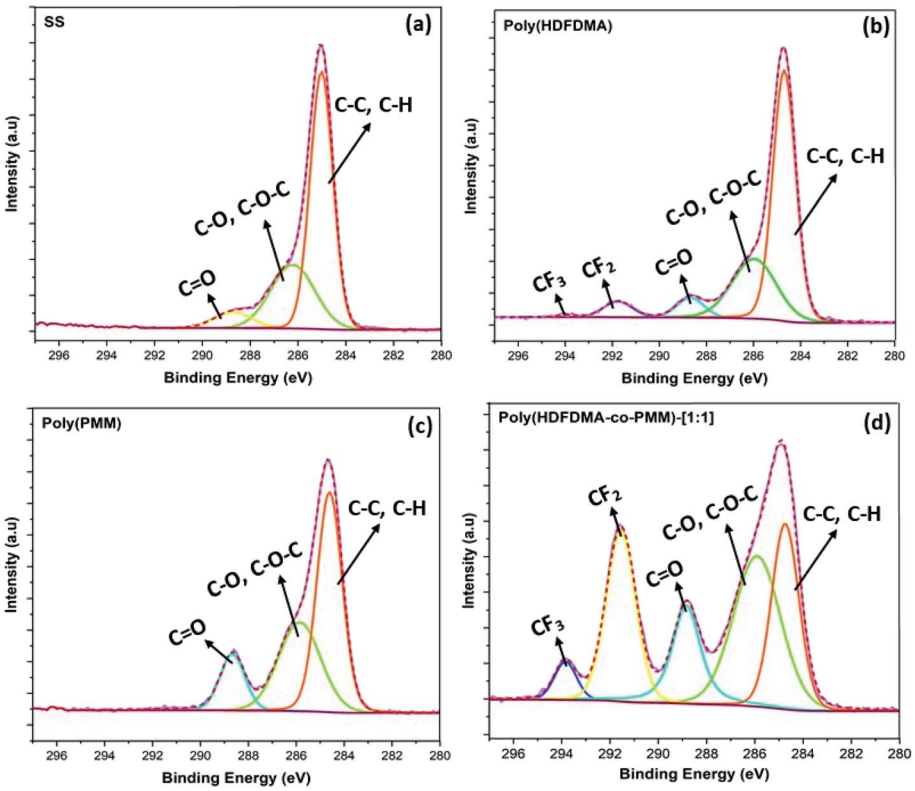

Fig. 7 (a) XPS core-level C 1s scans for uncoated, (b) poly(HDFDMA) homopolymer coated, (c) poly(PMM) homopolymer coated, and (d) poly(HDFDMA-*co*-PMM) copolymer with mol ratio [1 : 1] coated SS coupons. The purple solid line indicates the raw data line whereas the dotted line shows the peak fitting. The red color lines show the background.

possible components and their estimated fractions are listed in Table S2.† The C 1s spectrum of the uncoated SS with no surface coating (Fig. 7(a)) was deconvoluted into three distinct components.

The first major component, C 1s located at 285.0 eV corresponds to the carbon atom of C–C or C–H groups. The second one located at 285.8 eV is attributed to C–O or C–O–C groups and the third one located at 288.67 eV is ascribed to C═O.[51] The same deconvolution of the peaks was observed for the poly(PMM) homopolymer coated SS coupons. However, the C–C, C–H peak percentage composition decreases appreciably compared to the C–O and C═O (Fig. 7(c)) due to the ester groups of the methacrylates (Table S2†).

For fluorinated-polymer coated surfaces (poly(HDFDMA) and poly(HDFDMA-*co*-PMM)), the raw data were fitted into five peaks as shown in (Fig. 7(b and d)), with two new peaks for C 1s at 292 and 294 eV,[52] corresponding to $-CF_2-CF_2$ and $-CF_2-CF_3$ groups, respectively.[53]

These peaks are from the fluorinated components of the HDFDMA in the copolymer. The binding energies of the curve fittings result from the C 1s spectra of the uncoated and polymer coated surfaces are given in Table S3.† These peak assignments agreed well with previously reported values.[54,55]

The F/C atomic ratio and especially the concentration of the CF_3 groups of the copolymer with a mol ratio [1 : 1] was higher compared to other mol ratios and least for the homopolymer (poly(HDFDMA)) as can be seen from (Tables S2 and S3†). These data indicate that the lower surface free energy of the coatings from this mol ratio is attributed to the preferential enrichment of the surface with the CF_3 groups. As expected, a decrease in the elemental composition of CF_2 and CF_3 was observed with a decrease in fluorine contents as the mol ratio of fluorinated monomer decreased.

P 2p and F 1s core level scan

Further confirmation of the SS surface functionalization with the synthesized polymers was carried out by taking a close look into P 2p and F 1s spectra. The peak fitted high-resolution P 2p and F 1s spectra are shown in Fig. 8. The peak at around 133 eV, which can be deconvoluted of two peak components at a binding energy of 133.1–133.3 and 134.02–134.5 eV correspond to P $2p_{3/2}$ and P $2p_{1/2}$, respectively.

Similar peak assignments have been observed for 1*H*,1*H*,2*H*,2*H*-perfluorodecyl phosphonic acid on copper oxide surfaces.[56] However, Ishizaki *et al.*[53] assigned these two peaks to P–O–M and O═P–OH for magnesium alloy surfaces modified with *n*-octyl, *n*-dodecyl, *n*-octadecyl phosphonic acid, and 2-(perfluorohexyl)ethyl phosphonic acid. In this study, the peak for all other mol ratios of the copolymer is virtually unchanged and appears at similar binding energy regardless of the modifier, indicating similar binding modes and the formation of

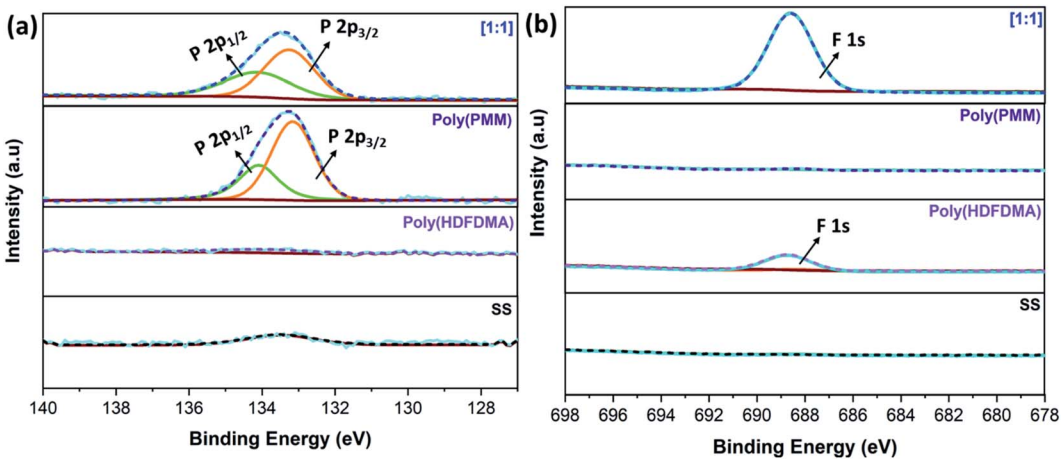

Fig. 8 (a) XPS core-level high resolution P 2p scans, and (b) F 1s scans, for uncoated, poly(HDFDMA) homopolymer coated, poly(PMM) homopolymer coated, and poly(HDFDMA-*co*-PMM) copolymer with mol ratio [1 : 1] coated SS coupon surfaces.

stable covalent bonds between the oxide surface and the deprotonated phosphonic acid headgroup[57,58] (Fig. S14(a)†).

On the other hand, no corresponding peak can be seen on the uncoated SS and poly(HDFDMA) fluorinated homopolymer coated surface. The binding energies (BE) that were obtained from the fitted peaks are presented in Table S3 in the ESI.† F 1s peak at 688 eV was attributed to C–F functional group which was observed in fluorinated polymers and absent in uncoated and poly(PMM) coated SS surfaces as expected (Fig. S14(b)†).

Furthermore, the carbon-to-phosphorus (C/P) and fluorine-to-phosphorus (F/P) ratios were calculated from the relative intensity of the elements and are summarized in Table 2. Fig. S15†, shows XPS high resolution O 1s spectra of (a) uncoated SS, (b) poly(PMM) coated SS, and (c) poly(HDFDMA-*co*-PMM) coated SS coupon surfaces. The O 1s spectra obtained for poly(PMM) show a very similar spectrum to the poly(-HDFDMA-*co*-PMM). The O 1s peak at 530.0 eV can be attributed to surface oxides (uncoated SS = 530.0 eV), and those at 531.8 eV are attributed to surface hydroxides (uncoated SS = 531.8) and P–O.[57,59] A peak at 533.8 eV attributable to P=O is observed in the spectra after the deposition of the polymer layer on the surface, which is inconsistent with tridentate phosphonate–surface bonding.[60,61]

Literature values for P=O groups are at BE 534.5–535 eV (ref. 60) in phosphonic and phosphoric acids on titania, while this BE was reported to be 532.1 eV in octadecylphosphoric acid on tantalum oxide.[62] This difference in BE might be due to different interactions with the stainless steel substrate with the P=O group. The O 1s data support that the polymers are covalently bound to the oxide or hydroxide surface of the SS surface in a monodentate or bidentate manner. From the above XPS analysis, it can be inferred that the anchoring of the homo- and co-polymers is *via* the phosphonate group.

Long-term stability

The stability of any adsorbed polymer film in water is important in any potential applications. The polymer coated SS coupons were tested for their stability by measuring the contact angle as a function of the immersion time for a period of up to 3 weeks. The measurements were carried out in triplicate after 4, 10, 15, and 21 days as shown in Fig. 9. Results revealed that CA dropped the least for poly(PMM),[63,64] and poly(HDFDMA-*co*-PMM) with mol ratios of [1 : 2], and [1 : 3] after 3 weeks of rinsing, indicating a strong binding of the phosphonic acids with the SS surface. All other polymer coated coupon surfaces dropped relatively more in CA suggesting a gradual loss of material.

These results are consistent with our previous work[14,44] where phosphonate based polymer layers have shown excellent stability upon rinsing under different rinsing conditions. Similar findings were observed in a recent study by Giamblanco

Table 2 The atomic percentage of elements from the XPS survey scan

Samples	C (%)	O (%)	P (%)	F (%)	Cr (%)	Fe (%)	F/P	F/C	C/P	P/C
SS	35.90	47.89	—	—	12.91	3.30	—	—	—	
Poly(HDFDMA)	45.92	35.26	—	8.68	8.79	1.35	—	0.18	—	
Poly(PMM)	41.06	45.93	3.86	—	6.76	2.39	—	—	10.64	0.094
[3 : 1]	39.48	38.00	1.53	10.65	9.02	1.32	6.96	0.27	25.80	0.04
[1 : 1]	42.52	20.92	2.14	30.98	2.34	1.1	14.47	0.74	19.86	0.05
[1 : 2]	45.53	26.57	3.67	20.13	2.54	1.56	5.48	0.44	12.40	0.08
[1 : 3]	44.36	28.00	3.32	19.3	3.34	1.68	5.81	0.44	13.36	0.074
[1 : 4]	46.49	31.36	3.08	14.51	2.85	1.71	4.71	0.32	15.09	0.098

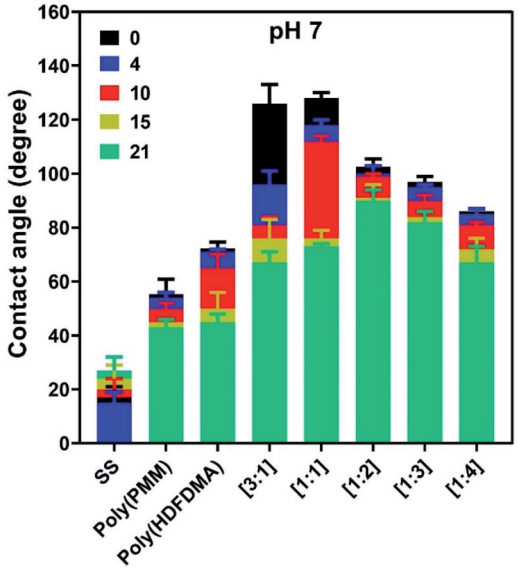

Fig. 9 Long-term stability study of homo and copolymers coated SS surfaces as measured by their static water angle (SCA) under the water rinsing conditions: neutral solution (pure water) along with uncoated SS (control). The SCA was measured after formation (black), rinsing after 4 days (blue), 10 days (red), 15 days (yellow), and 21 days (green) in the pure water. Data are presented as mean ± standard deviation (N = 3).

et al.[65] where they studied the stability of poly(ethylene glycol) copolymers with phosphonate units as surface tethering groups on an iron oxide surface in water, and the resultant films appeared stable. In another study, the stability of phosphonate based polymers on stainless steel was tested and the results showed strong covalent binding of phosphonates with stainless steel surfaces.[63]

All measurements were higher than the control SS coupon, which means that some polymer remained after this period in all the samples. The amount of polymer that desorbs will be a function of two main factors; the solubility of the polymer in water and its bonding to the metal oxide surface. The higher the fluorinated fraction, the lower the solubility will be in the water. On the other hand, the higher the phosphonate component, the stronger the expected binding. This can be observed in the results shown in Fig. 9. The highly fluorinated polymers lost a large fraction of their original contact angle due to less strong binding. The best results were found for the [1 : 2] copolymer which only lost about 11° in the CA measurements (from 102° to 91°), due to the best balance of binding and solubility. The layers deposited from DMSO followed the same stability trend as those from TFA (Fig. S10(b)†).

Experimental

Materials

1*H*,1*H*,2*H*,2*H*-Heptadecafluorodecyl methacrylate (CAS # 1996-88-9, catalog # 19226-25) was purchased from PolySciences, Inc (www.polysciences.com). (Dimethoxyphosphoryl)methyl methacrylate (DMPMM, CAS: 86242-61-7), was purchased from Specific Polymer, France. 2,2′-Azobis(isobutyronitrile) (AIBN, CAS: 78-67-1, 98%), trimethylsilyl bromide (TMS-Br, CAS: 2857-97-8, 97%), methanol (CH_3OH, CAS: 67-56-1, 99.8%), chloroform ($CHCl_3$, CAS: 67-66-3, 99.8%), trifluoroacetic acid (TFA, CAS: 76-05-1, 99%), trifluoroacetic acid-d (CF_3CO_2D, CAS: 599-00-8, 99% D), 1,1,1,3,3,3-hexafluoro-2-propanol (HFIP, CAS: 920-66-1, 95%) and phosphate-buffered saline (PBS; pH 7.4) in tablets were all purchased from Sigma-Aldrich. 1,4-Dioxane (AR grade) was purchased from VWR Chemicals. Chloroform-d ($CDCL_3$, CAS: 865-49-6, D, 99.8%) and deuterium oxide (D_2O, CAS: 7789-20-0, D, 99.9%) were purchased from Cambridge Isotope Laboratories, Inc. All pH adjustments were made with 1.0 mol L^{-1} HCl and NaOH. All starting materials were used without additional purification or modification. The water used for all surface experiments was from a water purification system (Milli-Q system; Millipore, 18.2 Ω).

Characterization methods

Nuclear magnetic resonance (NMR) spectroscopy. ^{1}H NMR, ^{31}P NMR, and ^{19}F NMR spectra were recorded using a Varian 400 MHz and 500 MHz NMR spectrometer at 298 K in either deuterated chloroform ($CDCl_3$), water (D_2O), or trifluoroacetic acid (CF_3CO_2D). The polymerization conversion was measured by ^{1}H NMR spectroscopy by comparing the signals of the reactive double bond (5.62 and 6.13 ppm) to the signals of the methylene in a-position of the phosphonated ester group at 4.14–4.47 ppm.

Gel permeation chromatography (GPC). The polymerization degree and molar mass dispersities (M_w/M_n) for all polymers were determined by gel permeation chromatography (PL-GPC 50, A Varian, Inc.) integrated GPC system (Chemistry Department, University of Otago). The GPC system was calibrated using narrow poly(ethylene oxide) (PEO) standards (EasyVial-Agilent). For protected polymers, high performance liquid chromatography grade $CHCl_3$ was used as a solvent. Polymers were dissolved in $CHCl_3$ and filtered through a 0.45 μm needle-type ultrafiltration membrane prior to the injection. The measurements were carried out at a flow rate of 1 mL min^{-1} and the molar masses were determined by refractive index detectors using a PEO–$CHCl_3$ calibration standard (Polymer Laboratories). The column temperature was set to 35 °C and Cirrus GPC software was used to analyze the data.

Thermogravimetric analysis (TGA). TGA was used to study the thermal stability of the synthesized homo and copolymers and was conducted on a Mettler Toledo TGA Q50 (TA Instruments). A sample of ≈20 mg was placed into a platinum pan and subjected to thermal degradation. Each sample was ramped from 20 to 700 °C at 5 °C min^{-1} in a nitrogen atmosphere. The remaining mass was recorded throughout the experiment as a function of temperature.

Cleaning of the SS surfaces. The stainless steel 316L coupons, 50 μm thick with 2B finish purchased from (www.allfoils.com) were cut in (2 × 2 cm) squares. Before surface modification, the coupons were cleaned using sulfochromic acid solution (20 mL H_2SO_4, 10 mL water, 0.5 g $K_2Cr_2O_7$ prepared at 40 °C for 5 min) for 2 minutes at room temperature

to remove organic contaminants, rinsed with water, and dried under a stream of nitrogen. **Caution**: handling of sulfochromic acid should be done in a fume hood, wearing gloves and goggles. Coupons were used immediately after the cleaning procedure.

Polymer immobilization. All fluorinated polymer solutions were prepared from 10 g L^{-1} stock solutions in trifluoroacetic acid (TFA), while poly(PMM) was prepared in pure water (pH 3.0) and dilutions were made at a concentration of 0.1 and 1 wt%. The clean SS coupons were immersed in a polymer solution. After 30 minutes of immersion, the coupons were rinsed three times with TFA followed by water to remove any weakly bound material and dried under a stream of nitrogen.

Static contact angles (SCA). Static contact angles were measured for all uncoated and polymer coated SS coupons using an FTÅ200 Goniometer apparatus (Data-Physics Instruments, University of Otago). Measurements were performed with water under open-air conditions at room temperature using the sessile droplet method. A drop of pure water (5 μL) was released from the Teflon tip of a syringe onto the sample surface for the static measurements. Digital images of the droplets were recorded after approximately 15 s. The average contact angle was calculated from 7 measurements at different locations on the coupon surface. All measurements were taken in triplicate for each coupon.

Attenuated total reflectance infrared (ATR-IR) spectroscopy. ATR-IR analysis of all polymer samples and SS coupon surfaces (uncoated and polymer coated) was carried out on a Bruker Alpha ATR-IR based spectrometer. The polymerization and copolymerization involved in the synthesis of polymers were primarily assessed using IR spectroscopy in the range of 4000–650 cm^{-1}.

X-ray photoelectron spectroscopy (XPS). The elemental surface composition of SS coupons before and after polymer coating was determined using XPS. XPS spectra were recorded on a Kratos Axis UltraDLD X-ray Photoelectron Spectrometer (Kratos Analytical, Manchester, UK) equipped with a hemispherical electron energy analyzer in ultra-high vacuum (UHV). Spectra were excited using monochromatic Al Kα X-rays (1486.69 eV) with the X-ray source operating at 150 W. All coupon samples were secured to the sample bar using double-sided carbon tape. This instrument illuminates a large area on the coupon surface and then using hybrid magnetic and electrostatic lenses collects photoelectrons from a desired location on the surface. In this case, the analysis area was a 300 by 700-micron spot obtained using the hybrid magnetic and electrostatic lens and the slot aperture. The survey scans were carried out in an energy range of 0–1300 eV with a pass energy of 80 eV, while the core level single spectra were collected using a pass energy of 20 eV and an acquisition time of 120 s. The binding energy (BE) was referenced to the C 1s photoelectron peak at 284.7 eV.[66] The deconvolution of high-resolution XPS peaks has been carried out by mixed Gaussian–Lorentzian fit after Shirley's background subtraction. Curve fitting and quantification were carried out using the CASAXPS processing software (Version 2.1.9).[67] XPS spectra of N 1s, was not fitted as the low intensities do not allow an accurate fitting. The estimated relative error of the XPS data is ±2%.

Long term stability tests. The stability of the polymer films formed on SS coupons was investigated in water under rinsing conditions using a static water contact angle goniometer. The SS coupons were coated with polymers (see polymer immobilization), rinsed, and dried under a stream of nitrogen. The dried coupons were transferred into separate vials, immersed in water, and placed in a shaking bath for the desired time period. Before each measurement, coupons were taken out from the solution, rinsed three times with water, and dried under nitrogen. Static contact angles were measured after 4, 10, 15, and 23 days by following the same procedure. All measurements were taken in triplicate for each coupon, and the results were averaged.

Homopolymerization of 1*H*,1*H*,2*H*,2*H*-heptadecafluorodecyl methacrylate

Heptadecafluorodecy methacrylate (HDFDMA) 1 g (1.87 mmol), and 2,2′-azobisisobutyronitrile (AIBN) 10 mg (0.06 mmol) were added in a Schlenk tube under argon along with 1,4-dioxane (7 mL). The mixture was degassed by three freeze–pump–thaw cycles prior to being placed in an oil bath. Afterward, the solution mixture was heated at 85 °C under argon in a thermostatic oil bath for an appropriate time. Samples were taken periodically for the determination of conversion (^{1}H NMR) and molar masses (GPC) analyses. The resultant polymer was isolated by precipitation into hexane, which was then filtered, and dried under reduced pressure yielding a fluffy solid (yield 84%).

Homopolymerization of (dimethoxyphosphoryl)methyl methacrylate

(Dimethoxyphosphoryl)methyl methacrylate (DMPMM, 1 g, 4.8 mmol), and 2,2′-azobisisobutyronitrile (AIBN) (10 mg, 0.06 mmol) were mixed and added to a Schlenk tube under argon along with 1,4-dioxane (6 mL). The reaction mixture was degassed by bubbling argon for 45 minutes and then heated at 85 °C under argon in a thermostatic oil bath for 24 h. Polymer conversions were determined by ^{1}H NMR and GPC analyses. The resulting poly(DMPMM) was purified by dialyzing in a membrane (MWCO: 3000–5000 Da) in water for 2 days and freeze-dried, yielding a colorless solid (85.4%).

Deprotection of phosphonate esters[25]

In a typical experiment, trimethylsilyl bromide (TMS-Br) (1.4 g, 9.42 mmol) was added to a solution of poly(DMPMM) (1 g, 0.062 mmol, M_n, GPC = 16 123 g mol^{-1}) in chloroform (20 mL). After stirring for 3 hours at room temperature, the mixture was concentrated under reduced pressure. Methanol (50 mL) was added and the mixture was stirred again for 1 hour at room temperature. The solvent was evaporated, and the product was dried to a constant weight under reduced pressure yielding a colorless solid (92%).

Copolymerization of HDFDMA and DMPMM

Typical polymerization procedure: HDFDMA (0.5 g, 0.94 mmol), DMPMM (0.19 g, 0.94 mmol), AIBN (0.005 g, 0.03 mmol) were added along with 1,4-dioxane (18 mL) in a Schlenk flask. The mixture was degassed by three freeze–evacuate–thaw cycles and then heated at 85 °C under argon in a thermostatic oil bath for 24 h. During the reaction, small samples were taken to measure the conversion. The resultant polymer was purified by adding water (20 mL) which was stirred for an hour, followed by filtration and drying under vacuum. The solid was dissolved in chloroform (50 mL) and stirred for 2 hours, and then re-precipitated in methanol. The copolymer was filtered and dried under a vacuum at room temperature overnight. The poly(HDFDMA-*co*-DMPMM) synthesized was a white solid with a 97% yield. This was deprotected into poly(HDFDMA-*co*-PMM) by using a similar procedure as used above (see deprotection of phosphonate esters). All synthesized homo and copolymers were characterized by ^{1}H, ^{31}P, ^{19}F NMR, GPC, ATR-TIR, and TGA analysis.

Statistical analysis

All experiments were performed in triplicate. For the sake of clarity, only one set of data is presented in this study in terms of graphs. However, very similar results were obtained for the other two sets of experiments. All data are presented as average $\pm$ standard error unless otherwise stated, and the statistical significance was assessed using the ANOVA test.

Conclusions

By using phosphonate groups, it is possible to graft fluorinated polymers onto stainless steel as a monolayer by simple immersion for 30 minutes from a dilute TFA or DMSO solution. The presence of the films on the surface was be shown by XPS, where peaks for both P and F atoms were detected. Initial contact angles of over 128° were measured for the most highly fluorinated films. This is higher than most simple fluoropolymers such as Teflon and may be aided by some surface roughness in the steel. The films showed good stability in water over a period of weeks, though some small loss of material was noted as inferred by the contact angle. The most stable films were from a polymer containing a [1 : 2] ratio of fluorinated to phosphonated monomers, which was ascribed to a balance between the number of binding sites in the polymer and its water solubility. The ease of application and the stability of the films makes this a promising technology for the synthesis of low surface energy metal surfaces.

Author contributions

FK conducted the formal analysis, investigation, visualization, and writing – original draft. SCM was involved in conceptualization, methodology, project administration, and supervision.

Conflicts of interest

There are no conflicts to declare.

Acknowledgements

We would like to thank the New Zealand Ministry of Business, Innovation, and Employment (MBIE) for funding the Biocide Tool Box (BTB) research program (UOAX1410). Author Farzana Kousar thanks the Biocide Tool Box for a PhD scholarship.

Notes and references

1 G. G. Hougham, P. E. Cassidy, K. Johns and T. Davidson, *Fluoropolymers 2*, 1999, vol. 2.
2 B. Ameduri, From vinylidene fluoride (VDF) to the applications of VDF-containing polymers and copolymers: recent developments and future trends, *Chem. Rev.*, 2009, **109**(12), 6632–6686.
3 S.-Y. Lu and I. Hamerton, Recent developments in the chemistry of halogen-free flame retardant polymers, *Prog. Polym. Sci.*, 2002, **27**(8), 1661–1712.
4 R. Ménard, C. Negrell, M. Fache, L. Ferry, R. Sonnier and G. David, From a bio-based phosphorus-containing epoxy monomer to fully bio-based flame-retardant thermosets, *RSC Adv.*, 2015, **5**(87), 70856–70867.
5 S. Monge, B. Canniccioni, A. Graillot and J.-J. Robin, Phosphorus-containing polymers: a great opportunity for the biomedical field, *Biomacromolecules*, 2011, **12**(6), 1973–1982.
6 M. Dadsetan, M. Giuliani, F. Wanivenhaus, M. B. Runge, J. E. Charlesworth and M. J. Yaszemski, Incorporation of phosphate group modulates bone cell attachment and differentiation on oligo (polyethylene glycol) fumarate hydrogel, *Acta Biomater.*, 2012, **8**(4), 1430–1439.
7 F. Millet, R. Auvergne, S. Caillol, G. David, A. Manseri and N. Pébère, Improvement of corrosion protection of steel by incorporation of a new phosphonated fatty acid in a phosphorus-containing polymer coating obtained by UV curing, *Prog. Org. Coat.*, 2014, **77**(2), 285–291.
8 A. Sannigrahi, S. Takamuku and P. Jannasch, Block selective grafting of poly(vinylphosphonic acid) from aromatic multiblock copolymers for nanostructured electrolyte membranes, *Polym. Chem*, 2013, **4**(15), 4207–4218.
9 C. Zhang, Y. Liu, S. Wen and S. Wang, Poly(vinylphosphonic acid) (PVPA) on titanium alloy acting as effective cartilage-like superlubricity coatings, *ACS Appl. Mater. Interfaces*, 2014, **6**(20), 17571–17578.
10 S. Monge and G. David, *Phosphorus-based polymers: from synthesis to applications*, RSC, 2014.
11 G. David, C. Negrell, A. Manseri and B. Boutevin, Poly(MMA)-*b*-poly(monophosphonic acrylate) diblock copolymers obtained by ATRP and used as additives for anticorrosive coatings, *J. Appl. Polym. Sci.*, 2009, **114**(4), 2213–2220.
12 Z. El Asri, K. Chougrani, C. Negrell-Guirao, G. David, B. Boutevin and C. Loubat, An efficient process for synthesizing and hydrolyzing a phosphonated

methacrylate: investigation of the adhesive and anticorrosive properties, *J. Polym. Sci. Pol. Chem*, 2008, **46**(14), 4794–4803.

13 A. R. Horrocks and S. Zhang, Enhancing polymer char formation by reaction with phosphorylated polyols. 1. Cellulose, *Polymer*, 2001, **42**(19), 8025–8033.

14 F. Kousar, J. Malmström, S. Swift, J. Ross, J. Perera and S. C. Moratti, Protein-Resistant Behavior of Poly(ethylene glycol)-Containing Polymers with Phosphonate/Phosphate Units on Stainless Steel Surfaces, *ACS Appl. Polym. Mater.*, 2021, **3**(5), 2785–2801.

15 B. Ameduri and B. Boutevin, *Well-architectured fluoropolymers: synthesis, properties and applications*, Elsevier, 2004.

16 A. L. Moore and J. G. Drobny, *Fluoroelastomers handbook: the definitive user's guide and databook*, Taylor & Francis, 2006.

17 F. Boschet and B. Ameduri, (Co) polymers of chlorotrifluoroethylene: synthesis, properties, and applications, *Chem. Rev.*, 2014, **114**(2), 927–980.

18 B. Ameduri, G. Bauduin, B. Boutevin, G. Kostov and P. Petrova, Synthesis and polymerization of fluorinated monomers bearing a reactive lateral group. 9 bulk copolymerization of vinylidene fluoride with 4,5,5-trifluoro-4-ene pentyl acetate, *Macromolecules*, 1999, **32**(14), 4544–4550.

19 A. Kraytsberg and Y. Ein-Eli, Review of advanced materials for proton exchange membrane fuel cells, *Energy Fuels*, 2014, **28**(12), 7303–7330.

20 S. Banerjee, *Handbook of specialty fluorinated polymers: Preparation, Properties, and Applications*, William Andrew, 2015.

21 A. Taguet, B. Ameduri and B. Boutevin, Crosslinking of vinylidene fluoride-containing fluoropolymers, *J. Mater. Sci.*, 2005, 127–211.

22 M. N. Wadekar, Y. R. Patil and B. Ameduri, Superior Thermostability and Hydrophobicity of Poly (vinylidene fluoride-co-fluoroalkyl 2-trifluoromethacrylate), *Macromolecules*, 2014, **47**(1), 13–25.

23 E. Bayer, P. A. Grathwohl and K. Geckeler, Poly (vinylalcohol) as polymeric support for metal chelating phosphoric acid and derivatives, *Macromol. Chem. Phys.*, 1983, **113**(1), 141–152.

24 C. R. Nair, G. Clouet and J. Brossas, Copolymerization of diethyl 2-(methacryloyloxy) ethyl phosphate with alkyl acrylates: Reactivity ratios and glass transition temperatures, *J. Polym. Sci. Pol. Chem*, 1988, **26**(7), 1791–1807.

25 B. Canniccioni, S. Monge, G. David and J.-J. Robin, RAFT polymerization of dimethyl (methacryloyloxy) methyl phosphonate and its phosphonic acid derivative: a new opportunity for phosphorus-based materials, *Polym. Chem*, 2013, **4**(13), 3676–3685.

26 R. Boissezon, J. Muller, V. Beaugeard, S. Monge and J.-J. Robin, Organophosphonates as anchoring agents onto metal oxide-based materials: synthesis and applications, *RSC Adv.*, 2014, **4**(67), 35690–35707.

27 N. Zhang, S. Salzinger and B. Rieger, Poly(vinylphosphonate) s with widely tunable LCST: a promising alternative to conventional thermoresponsive polymers, *Macromolecules*, 2012, **45**(24), 9751–9758.

28 G. David, C. Negrell-Guirao, F. Iftene, B. Boutevin and K. Chougrani, Recent progress on phosphonate vinyl monomers and polymers therefore obtained by radical (co) polymerization, *Polym. Chem*, 2012, **3**(2), 265–274.

29 C. M. Timperley, R. E. Arbon, M. Bird, S. A. Brewer, M. W. Parry, D. J. Sellers and C. R. Willis, Bis(fluoroalkyl) acrylic and methacrylic phosphate monomers, their polymers and some of their properties, *J. Fluorine Chem.*, 2003, **121**(1), 23–31.

30 R. Tayouo, G. David, B. Ameduri, J. Roziere and S. Roualdes, New fluorinated polymers bearing pendant phosphonic acid groups. Proton conducting membranes for fuel cell, *Macromolecules*, 2010, **43**(12), 5269–5276.

31 S. Banerjee, M. Wehbi, A. Manseri, A. Mehdi, A. Alaaeddine, A. Hachem and B. Ameduri, Poly(vinylidene fluoride) containing phosphonic acid as anticorrosion coating for steel, *ACS Appl. Mater. Interfaces*, 2017, **9**(7), 6433–6443.

32 E. Labalme, G. David, P. Buvat and J. Bigarre, A simple strategy based on a highly fluorinated polymer blended with a fluorinated polymer containing phosphonic acid to improve the properties of PEMFCs, *New J. Chem.*, 2019, **43**(28), 11141–11147.

33 J. Lee, H. S. Hwang, W.-G. Koh and I. Park, Robust and superomniphobic core-shell SiO2@poly(1H,1H,2H,2H-heptadecafluorodecyl methacrylate-co-methyl methacrylate) coating materials synthesized by thiol lactam initiated radical polymerization, *Prog. Org. Coat.*, 2020, **148**, 1–9.

34 M. Sohail, B. Ashfaq, I. Azeem, A. Faisal, S. Y. Doğan, J. Wang, H. Duran and B. Yameen, A facile and versatile route to functional poly(propylene) surfaces *via* UV-curable coatings, *React. Funct. Polym.*, 2019, **144**, 1–14.

35 D. L. Schmidt, R. F. Brady, K. Lam, D. C. Schmidt and M. K. Chaudhury, Contact angle hysteresis, adhesion, and marine biofouling, *Langmuir*, 2004, **20**(7), 2830–2836.

36 J. Shin, W. Bae, Y.-W. Lee and H. Kim, Kinetics for free radical solution polymerization of heptadecafluorodecyl (meth)acrylate in supercritical carbon dioxide, *Korean J. Chem. Eng.*, 2007, **24**(4), 664–669.

37 J. Shin, Y.-W. Lee, H. Kim and W. Bae, High-pressure phase behavior of carbon dioxide+ heptadecafluorodecyl acrylate+ poly(heptadecafluorodecyl acrylate) system, *J. Chem. Eng. Data*, 2006, **51**(5), 1571–1575.

38 X. Solimando, E. Kennedy, G. David, P. Champagne and M. F. Cunningham, Phosphorus-containing polymers synthesised *via* nitroxide-mediated polymerisation and their grafting on chitosan by grafting to and grafting from approaches, *Polym. Chem*, 2020, **11**(25), 4133–4142.

39 J. Norman, S. Moratti, A. Slark, D. Irvine and A. Jackson, Synthesis of Well-Defined Macromonomers by Sequential ATRP^{-} Catalytic Chain Transfer and Copolymerization with Ethyl Acrylate, *Macromolecules*, 2002, **35**(24), 8954–8961.

40 L. Yao, T. Yang and S. Cheng, Synthesis and characterization of poly(fluorinated acrylate)/silica hybrid nanocomposites, *J. Appl. Polym. Sci.*, 2010, **115**(6), 3500–3507.
41 K. Li, P. Wu and Z. Han, Preparation and surface properties of fluorine-containing diblock copolymers, *Polymer*, 2002, **43**(14), 4079–4086.
42 S. V. Kotov, S. D. Pedersen, W. Qiu, Z.-M. Qiu and D. J. Burton, Preparation of perfluorocarbon polymers containing phosphonic acid groups, *J. Fluor. Chem*, 1997, **82**(1), 13–19.
43 M. Yamabe, K. Akiyama, Y. Akatsuka and M. Kato, Novel phosphonated perfluorocarbon polymers, *Eur. Polym. J.*, 2000, **36**(5), 1035–1041.
44 F. Kousar, *Modification of stainless steel by grafting of poly(ethylene glycol) copolymers for reduction in protein adsorption and bacterial adhesion*, University of Otago, 2021.
45 Y. Xiao, L. Zhao, Y. Shi, N. Liu, Y. Liu, B. Liu, Q. Xu, C. He and X. Chen, Surface modification of 316L stainless steel by grafting methoxy poly(ethylene glycol) to improve the biocompatibility, *Chem. Res. Chin. Univ.*, 2015, **31**, 651–657.
46 H. Fox and W. Zisman, The spreading of liquids on low energy surfaces. I. polytetrafluoroethylene, *J. Colloid. Sci*, 1950, **5**(6), 514–531.
47 J. Drelich, J. D. Miller and R. J. Good, The effect of drop (bubble) size on advancing and receding contact angles for heterogeneous and rough solid surfaces as observed with sessile-drop and captive-bubble techniques, *J. Colloid Interface Sci.*, 1996, **179**(1), 37–50.
48 F. Fowkes, D. McCarthy and M. Mostafa, Contact angles and the equilibrium spreading pressures of liquids on hydrophobic solids, *J. Colloid Interface Sci.*, 1980, **78**(1), 200–206.
49 M. A. Nilsson, R. J. Daniello and J. P. Rothstein, A novel and inexpensive technique for creating superhydrophobic surfaces using Teflon and sandpaper, *J. Phys. D. Apply. Phys*, 2010, **43**(4), 045301.
50 S. Tang, N. Lu, S.-W. Myung and H.-S. Choi, Enhancement of adhesion strength between two AISI 316 L stainless steel plates through atmospheric pressure plasma treatment, *Surf. Coat. Technol.*, 2006, **200**(18–19), 5220–5228.
51 I. Al-Hamarneh, P. Pedrow, A. Eskhan and N. Abu-Lail, Hydrophilic property of 316L stainless steel after treatment by atmospheric pressure corona streamer plasma using surface-sensitive analyses, *Appl. Surf. Sci.*, 2012, **259**, 424–432.
52 J. Moulder, W. Stickle, F. Sobol and D. Bomben, *Phys. Electron.*, 1995, 230–232.
53 T. Ishizaki, K. Teshima, Y. Masuda and M. Sakamoto, Liquid phase formation of alkyl-and perfluoro-phosphonic acid derived monolayers on magnesium alloy AZ31 and their chemical properties, *J. Colloid Interface Sci.*, 2011, **360**(1), 280–288.
54 I. J. Park, S. B. Lee and C. K. Choi, Surface properties for poly (perfluoroalkylethyl methacrylate)/poly(*n*-alkyl methacrylate) s mixtures, *J. Appl. Polym. Sci.*, 1994, **54**(10), 1449–1454.
55 R. Van de Grampel, W. Ming, A. Gildenpfennig, W. Van Gennip, J. Laven, J. Niemantsverdriet, H. Brongersma, G. De With and R. Van der Linde, The outermost atomic layer of thin films of fluorinated polymethacrylates, *Langmuir*, 2004, **20**(15), 6344–6351.
56 E. Hoque, J. DeRose, B. Bhushan and K. Hipps, Low adhesion, non-wetting phosphonate self-assembled monolayer films formed on copper oxide surfaces, *Ultramicroscopy*, 2009, **109**(8), 1015–1022.
57 J. Rechmann, A. Sarfraz, A. C. Götzinger, E. Dirksen, T. J. Müller and A. Erbe, Surface functionalization of oxide-covered zinc and iron with phosphonated phenylethynyl phenothiazine, *Langmuir*, 2015, **31**(26), 7306–7316.
58 T. Keszthelyi, Z. Pászti, T. Rigó, O. Hakkel, J. Telegdi and L. Guczi, Investigation of solid surfaces modified by Langmuir–Blodgett monolayers using sum-frequency vibrational spectroscopy and X-ray photoelectron spectroscopy, *J. Phys. Chem.*, 2006, **110**(17), 8701–8714.
59 P. Thissen, M. Valtiner and G. Grundmeier, Stability of phosphonic acid self-assembled monolayers on amorphous and single-crystalline aluminum oxide surfaces in aqueous solution, *Langmuir*, 2010, **26**(1), 156–164.
60 C. Viornery, Y. Chevolot, D. Léonard, B.-O. Aronsson, P. Péchy, H. J. Mathieu, P. Descouts and M. Grätzel, Surface modification of titanium with phosphonic acid to improve bone bonding: characterization by XPS and ToF-SIMS, *Langmuir*, 2002, **18**(7), 2582–2589.
61 A. Raman, M. Dubey, I. Gouzman and E. S. Gawalt, Formation of self-assembled monolayers of alkylphosphonic acid on the native oxide surface of SS316L, *Langmuir*, 2006, **22**(15), 6469–6472.
62 M. Textor, L. Ruiz, R. Hofer, A. Rossi, K. Feldman, G. Hähner and N. D. Spencer, Structural chemistry of self-assembled monolayers of octadecylphosphoric acid on tantalum oxide surfaces, *Langmuir*, 2000, **16**(7), 3257–3271.
63 M. Kosian, M. M. Smulders and H. Zuilhof, Structure and long-term stability of alkylphosphonic acid monolayers on SS316L stainless steel, *Langmuir*, 2016, **32**(4), 1047–1057.
64 A. Debrassi, A. Ribbera, W. M. de Vos, T. Wennekes and H. Zuilhof, Stability of (bio) functionalized porous aluminum oxide, *Langmuir*, 2014, **30**(5), 1311–1320.
65 N. Giamblanco, G. Marletta, A. Graillot, N. Bia, C. Loubat and J.-F. o. Berret, Serum protein-resistant behavior of multisite-bound poly(ethylene glycol) chains on iron oxide surfaces, *ACS omega*, 2017, **2**(4), 1309–1320.
66 J. Moulder and W. Stickle and P. Sobol, *Handbook of X-ray Photoelectron Spectroscopy*, Perkin-Elmer Corp., Eden Prairie, MN, USA, 1992.
67 E. Hoque, J. DeRose, P. Hoffmann, H. Mathieu, B. Bhushan and M. Cichomski, Phosphonate self-assembled monolayers on aluminum surfaces, *J. Chem. Phys.*, 2006, **124**(17), 174710.